Structural modifications in bismuth cuprates: Effects on the electronic structure and Fermi surface

D. J. Singh and W. E. Pickett
Complex Systems Theory Branch, Naval Research Laboratory, Washington, D.C. 20375-5345
(Received 30 September 1994)

We compare the electronic structure of the idealized tetragonal model of $Bi_2Sr_2CuO_6$ with that of the more realistic orthorhombic $\sqrt{2}\times\sqrt{2}$ cell as determined by Torardi and collaborators. The distortions, which involve atomic displacements as large as 0.45 Å, shift the Bi-O(3) derived bands at the Fermi level strongly, and change the number of Fermi surfaces and their topology. We emphasize that such complications, which are probably even larger in $Bi_2Sr_2CaCu_2O_8$, must be taken into acount in the interpretation of angle-resolved photoemission spectroscopy (ARPES), since we find for this compound several Fermi surfaces in the region of the $\bar{M}$ point where flat bands are seen in ARPES data. These effects will also affect the interpretation of the measured superconducting energy gap over the Fermi surface(s).

I. INTRODUCTION

One of the most active areas in the study of high-temperature superconductors (HTS) currently is spectroscopy at and near the Fermi surface, in the expectation of gaining knowledge of the character of the quasiparticles and the size and symmetry of the superconducting energy gap. The observation of a Fermi edge and of spectral peaks dispersing through the Fermi surface allows the mapping of a number of the properties most fundamental to furthering our understanding of high-temperature superconductivity, viz., Fermi surfaces and carrier velocities, effective masses, superconducting gap. The mapping of the Fermi surface has been the most extensive and least ambiguous in $YBa_2Cu_3O_7$,[1] but the opening of the superconducting gap has not been observed with photoemission in this compound (apparently because the surface layer is not superconducting).

Another widely studied HTS cuprate is $Bi_2Sr_2CaCu_2O_8$ (Bi2212), which cleaves readily. Due in large part to the ease in observing the opening of an energy gap below the superconducting critical temperature T_c, the Bi2212 phase has been the focus of much attention. Dispersing spectral features are observed, and the opening of a gap below T_c has been reported by several groups.[2–8] Two aspects of these data have been the focus of attention: (1) to what extent do the bands agree or disagree with local-density-approximation (LDA) band-structure calculations and (2) can one surmise the gap symmetry from the data? At present there is strong disagreement at least in part because the underlying data vary considerably from group to group (or with sample preparation).

One aspect of the bismuth cuprates that has been virtually ignored in the interpretation of the spectroscopic data is the incommensurate superstructure, which greatly complicates the interpretation of the data. It is unknown at present to what extent the superstructure also complicates comparison with band-structure results, which are carried out on simpler structural models. Several structural studies have shown that the displacements of atoms from idealized positions are large in the Bi-O layers of the cell (several tenths of an Angstrom), involve z-axis modulations as well as planar displacements, and even extend to the Cu-O layers of the cell.[9–18]

LDA electronic structures were reported[19–23] shortly after the discovery of bulk superconductivity in the materials. Such results have been used extensively in comparison with experimental data, particularly for Bi2212. However, the calculations were necessarily based on simple structural models, i.e., body-centered tetragonal with one formula unit per cell. As such, effects of structural distortions were neglected. Herman, Kasowski, and Hsu[24] reported band structures for Bi2212 with a simple tetragonal structure similar to that of Refs. 19–23 as well as with a model containing displacements of the Bi and O atoms and found significant shifts in the bands. Unfortunately, their band structure differs greatly from those obtained by other workers, having, for example, extra Cu-O derived Fermi surfaces other than the barrel sections.

Here we study the effects of structural distortions in the one Cu-O layer bismuth cuprate $Bi_2Sr_2CuO_6$ (Bi2201). This compound was chosen because it is simpler than Bi2212 but contains the same important Bi-O layers [the Bi layer oxygen will be designated O(3)], and because there is a relatively simple $\sqrt{2}\times\sqrt{2}$ superstructure that reasonably approximates the actual (incommensurate) structure.[25] There is a corresponding $\sqrt{2}\times\sqrt{2}$ structural model in Bi2212, but stronger modulation and unequal concentrations of Bi and O(3) likely make the $\sqrt{2}\times5\sqrt{2}$ structure the simplest reasonable analog. We find that the orthorhombic displacements in Bi2201 lead to substantial shifts of hundreds of meV in the bands with significant Bi-O character, which occur around the Fermi energy. This results in important changes in the Fermi surfaces that are well above experimental resolution and depart from the square symmetry that is commonly assumed (but often not observed). The implication is that band-structure calculations based on idealized structural models of Bi2212 should not be relied upon in detail in the interpretation of spectral data, and conversely that tetragonal symmetry should not be assumed and data over the full orthorhombic zone ought to be gathered.

II. METHOD

The present calculations were performed using the general potential linearized augmented plane-wave (LAPW) method.[26,27] A local orbital extension[28] was used to accurately treat the high-lying extended core states and to relax any linearization errors. Well-converged basis sets consisting of approximately 3100 functions were used in the doubled $\sqrt{2}\times\sqrt{2}$ cell.[29,30] Self-consistency was obtained using eight special **k** points in the irreducible wedge of the zone (IBZ), while the Fermi energy, electronic density of states, and Fermi surfaces are based on 81 **k** points in the IBZ. Spin-orbit effects were included through a second variational procedure. In order to isolate the effects of the modulation, parallel calculations were performed for a simplified body-centered-tetragonal structural model (TET) similar to that of Sterne and Wang.[21] This was constructed by moving ions parallel to the plane of the CuO_2 sheet into positions consistent with the tetragonal symmetry and setting the **a** lattice parameter to the geometric mean of the orthorhombic **a** and **b** parameters.

III. STRUCTURES

Although, like Bi2212, the Bi2201 compound contains an incommensurate superstructure, it is less severe. Torardi *et al.*[25] have approximated it with an orthorhombic cell of space group *Amaa* (No. 66, nonconventional setting of *Cccm*), with cell parameters $a=5.362$ Å, $b=5.374$ Å, $c=24.622$ Å and two formula units per primitive cell. Aside from the small orthorhombic distortion of 0.2%, the structure can be considered as a distorted $\sqrt{2}\times\sqrt{2}$ version of a tetragonal cell whose planar axes lie along the Cu-O bonds, and whose x- and y-atomic positions are all determined by symmetry. We refer to this idealized cell as the TET structure, with the more realistic orthorhombic structure of Torardi *et al.* being called the ORTH cell. We find that the total energy of the ORTH structure is 0.68 eV per formula unit lower than that of the TET structure, supporting the notion that the TET structure is far from realistic for Bi2201 and leading to the expectation that the electronic structures of the two models could differ significantly.

The primary distortions in the ORTH cell lie along the orthorhombic b axis, which is (nearly) 45° with respect to the Cu-O bonds. The Bi atoms are displaced by 0.14 Å and the O(3) atoms in the Bi layer (see below) are displaced by 0.45 Å. The Sr atom and the O(2) atom in its layer (the apical O) are displaced by -0.01 and 0.13 Å, respectively. Due to these displacements the Bi, Sr, O(3), and O(2) atoms lie at sites of only mirror symmetry (in the a-c plane).

The Cu and O(1) atoms retain their normal high-symmetry x and y coordinates. There are also identifiable distortions along the z axis, in the sense that the cations and anions are not coplanar; these are included in both the TET and ORTH structural models. The Bi and O(3) heights are different by 0.05 Å, the Sr and O(2) layers are separated by 0.84 Å, and even the O(1) atoms lie ± 0.10 Å above and below the Cu layer.

This structure for Bi2201 has CuO_6 octahedra typical of many cuprates, but they are tilted alternately in a direction at 45° from the Cu-O bonds (analogous to the orthorhombic distortion in La_2CuO_4). The rocksalt arrangement of Bi and O(3) atoms in the TET structure is modified by the alternating displacement of lines of both Bi atoms and O(3) atoms such the uniform Bi-O(3) distances of $a/2=2.68$ Å become distances of 2.68 ± 0.59 Å along the b axis, and two equal separations of 2.70 Å along the a axis.

It should be noted that the O(3) and O(2) atoms, followed by the Bi atom, have the largest "thermal factors" in the structural refinement, so the remaining incommensurate distortions affect primarily these atoms. These incommensurations have been modeled by Heinrich *et al.*[31] Although we have included the orthorhombic distortion in our calculations for the ORTH structure, it is very small and apparently unimportant, hence we will ignore it in our discussions below.

IV. TET Bi2201

The band structure of TET Bi2201 is displayed in Fig. 1. The bands crossing E_F are a Cu-O derived barrel band, which is characteristic of the HTS cuprates and crosses E_F along the Γ-X and Z-X directions, as well as two Bi-O derived bands dipping below E_F near the midpoint of the long Γ-Z direction. A Cu-O derived band approaches E_F from below in this same region and mixes with the Bi-O bands. The weak dispersion of the bands perpendicular to the CuO_2 plane is reflected in the small deviations from mirror symmetry along the long Γ-Z line about its midpoint and along the Z-X-Γ path about the X point as well as the weak dispersions along the short Γ-Z direction.

This picture of the TET band structure is qualitatively similar to that obtained by Sterne and Wang, but there

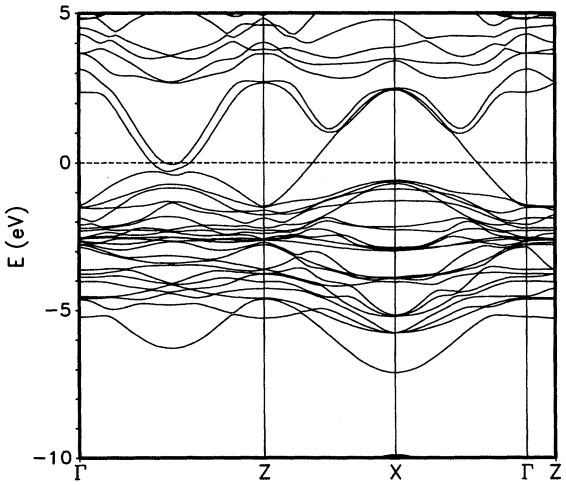

FIG. 1. Band structure of TET Bi2201. Note that the long Γ-Z line in the body-centered-tetragonal zone lies in the basal ($\mathbf{k}_x=0$) plane. If there were no z-axis dispersion the bands along this line would be symmetric about its midpoint. The horizontal dashed line denotes the Fermi energy.

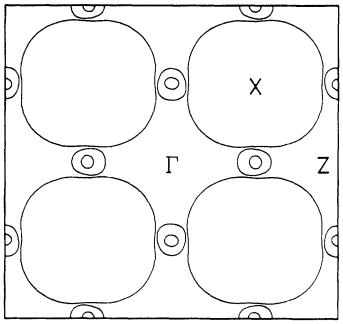

FIG. 2. Fermi surfaces of TET Bi2201 in the basal ($\mathbf{k}_z=0$) plane. Γ points are at the corners and center of the plot, while the edge centers are Z points.

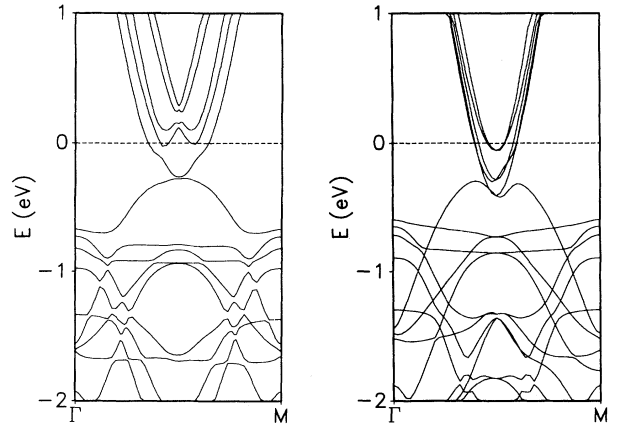

FIG. 3. Band structure of ORTH Bi2201 along the Γ-M, $[2\alpha,-\alpha,\alpha]$ line in reciprocal-lattice coordinates (left panel) and the corresponding folded TET Bi2201 band structure (right panel) which consists of the long TET Γ-Z line and a zone boundary line from $[\frac{1}{2},\frac{1}{2},\frac{1}{2}]$ to $[-\frac{1}{2},\frac{1}{2},0]$. The horizontal dashed line denotes the Fermi energy.

are quantitative differences. These are of roughly the same size as differences between their calculation and the LAPW calculations of Krakauer and Pickett[20] for tetragonal Bi2212 and are presumably due to their use of the linearized muffin-tin orbital method within the atomic-spheres approximation (LMTO-ASA), which is significant for materials with open structures and low site symmetries like the HTS.

Calculated Fermi surfaces of TET Bi2201 are displayed in Fig. 2. They consist of three cylindrical sections corresponding to the three bands crossing E_F. These are a large Cu-O derived barrel section centered at X and two small Bi-O derived hole cylinders centered at the midpoints of the long Γ-Z directions (on a per cell basis there is one CuO barrel and two each of the two Bi-O cylinders). The very weak z-axis dispersion of the electronic structure near E_F is reflected in the fact that the Fermi surfaces are nearly identical as viewed from the Γ and Z points. The two concentric Bi-O cylinders together contain a volume of 6% of the zone, which would correspond to a hole doping level of 0.12 holes per Cu ion. This is very similar to the doping level per Cu ion calculated from tetragonal Bi2212,[19,20] although in this case only one of the two Bi-O bands crosses E_F. However, because of the larger size of the single Bi-O derived cylinders in Bi2212 the hybridization with and resulting distortion of the Cu-O derived barrels in its vicinity is much stronger in that material.

V. ORTH Bi2201

A. Band structure

In TET Bi2201 Bi-O derived bands expected to be most strongly affected by the superstructure modulation approach E_F near the midpoints of the long Γ-Z directions. Accordingly, we initially focus on the band structure near E_F in this region. The corresponding direction is $[2\alpha,-\alpha,\alpha]$ from Γ to $[1,-\frac{1}{2},\frac{1}{2}]$ (reciprocal-lattice coordinates). For convenience we denote this line, which lies in the basal plane, as Γ-M;[30] note that the two-dimensional (2D) $\bar{M}$ point lies at the midpoint of this line. The band structure for ORTH Bi2201 along this direction is shown in Fig. 3 along with the equivalent folded band structure for TET Bi2201. Five bands approach E_F near the midpoint of the Γ-M line. Four are Bi-O derived bands, corresponding to the two shown in Fig. 1 along Γ-Z and two others from the zone boundary $[\frac{1}{2},\frac{1}{2},\frac{1}{2}]$ (X point which folds to Γ to the ORTH zone) to the $[-\frac{1}{2},\frac{1}{2},0]$ line. The fifth band near E_F arises from crossing the Cu-O derived barrel Fermi surfaces along the zone boundary line (see Fig. 2).

It is apparent from the plot that these five bands are strongly affected near the midpoint of the Γ-M line by the superstructure displacement. The four bands corresponding the Bi-O Fermi surfaces are shifted upward by approximately 400 meV near E_F, and as a result only one of the four now crosses E_F along this line. The fifth (outer) band near E_F becomes lower and takes a weaker dispersion (heavier mass). These differences are well above the resolution of angle-resolved photoemission spectroscopy (ARPES) techniques.

The upward shifts of the Bi-O bands resulting from the atomic distortions are qualitatively like those discussed by Ren *et al.*[32] However, because they used non-self-consistent empirical parameters and did not treat the interaction with the Cu-O bands, they obtained considerably larger shifts that are not borne out by the present self-consistent results.

B. Fermi surfaces

Figure 4 shows the Fermi surfaces for TET Bi2201 folded into the doubled ORTH zone and rotated by 45°, along with those of ORTH Bi2201 to allow direct comparison. As mentioned, the TET Bi2201 Fermi surfaces consist of the usual Cu-O barrel Fermi surface and two small quasicylindrical electron rods arising from the Bi-O(3) bands. There is hybridization in the region of near contact.

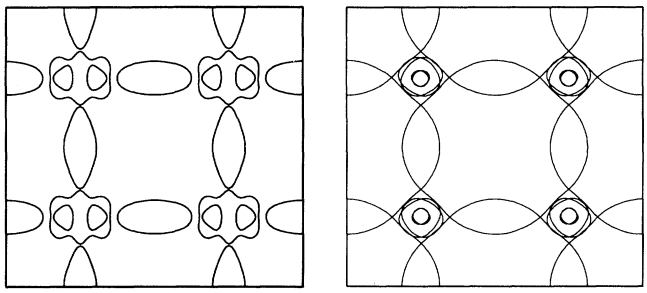

FIG. 4. Basal plane Fermi surfaces of ORTH Bi2201 (left panel) and TET Bi2201 folded into the same zone (right panel). The vertical direction is along $[\alpha,0,0]$ while the horizontal is $[0,-\beta,\beta]$ in reciprocal-lattice units. Γ points are at the corners and the midpoints of the horizontal edges. Note that the ORTH zone is rotated 45° with respect to the TET zone.

In the doubled ORTH zone the holelike barrel Fermi surface is centered at Γ. It roughly fills the BZ in area and its rounded corners overlap with those of barrels from neighboring Brillouin zones. The displacements in ORTH Bi2201 cause considerable changes in the Fermi surface: the overlapping regions of the barrels become large lenses that are slightly separated from distorted rectangular Fermi surface containing two rods that are rounded triangles in cross section. However, the Fermi surfaces can be pictured more simply as overlapping Cu-O(1) barrel surfaces that also overlap with two Bi-O(3) lenses that are split away from the midpoints of the Γ-M lines along the a direction. The small breaks in the barrel Fermi surfaces near the Bi-O sections would be physically meaningful only in highly perfect crystals, which the bismuth cuprates are not. In any case, observation of such breaks requires better angular resolution than is now possible in ARPES experiments. It is, however, very important to observe that throughout this region, which amounts to 20% of the zone, there are bands within 125 meV of E_F. The complexity of these bands, which have considerable Bi-O derived character, may be further perturbed by the incommensurate modulation present in the Bi-O layer, but not included in our model for ORTH Bi2201. These bands, their complex dispersions, and their proximity to E_F may explain the great difficulty in mapping out the electronic structure in this part of the zone via ARPES.

C. Density of states

As may be expected from the relatively large effects of the ORTH Bi-O displacements on the band structure and Fermi surfaces, the electronic density of states (DOS) near E_F is also affected by the modulation. The total and atom-decomposed DOS for the TET and ORTH structures are shown in Fig. 5. Differences in detail are visible throughout the bands, particularly the critical point structures that are sensitive to symmetry. The most notable changes in going from the TET to ORTH structures are (i) the strong decrease in the Bi DOS at E_F, and (ii) the shift in O(3) spectral density around -0.1 to -0.2 Ry to higher binding energy. The near complete suppression of Bi-O(3) derived character at E_F in ORTH Bi2201 is particularly striking. It results in a reduction in the total DOS at E_F $[N(E_F)]$, which includes the CuO_2 barrel contribution, from 19.6 states/Ry for TET Bi2201 to 13.3 states/Ry on a per formula unit basis.

A simple estimate of the doping level for the ORTH structure based on Fermi surface areas is complicated by the breaks in the Fermi surfaces and the associated hybridization of Bi-O derived and Cu-O derived components. Nonetheless, some qualitative remarks may be made. The Bi-O(3) contribution to the DOS is shifted upwards resulting in less Bi-O derived character below E_F. This is consistent with the observed upward shift in the Bi-O(3) derived band structure near E_F and the reduction in the number and size of the Bi-O(3) related Fermi surfaces. This corresponds to a lower occupancy of the Bi-O(3) states, and accordingly higher occupancy of Cu-O derived states, i.e., a lower hole doping level than for the TET structure. Moreover, the magnitude of the shifts suggest that the doping level may be considerably lower than the 0.12 holes per Cu ion obtained for the TET structure, and this may be responsible for the depressed critical temperature in Bi2201.

VI. SUMMARY AND DISCUSSION

The above LDA electronic structure calculations for tetragonal Bi2201 and a simple $\sqrt{2}\times\sqrt{2}$ orthorhombic model of the incommensurate modulated Bi-O displacements, show that the displacements strongly affect the electronic structure near E_F. Bi-O derived bands are shifted by as much as 400 meV and the size, shape, and number of Bi-O derived Fermi surfaces is changed. Including the modulation, Bi-O derived bands occur within 125 meV of E_F in a large region amounting to 20% of the zone, centered along the midpoint of the (1,1) Γ-M line. Such a complex of bands near E_F is consistent with recent measurements. In particular, Ratner *et al.*[33] and more recently, King *et al.*[34] have reported ARPES data for $Bi_2(Sr_{1-x}Pr_x)CuO_{6+\delta}$, $x=0.03-0.05$, that show states near E_F throughout the region near $\bar{M}$ where the Bi-O bands lie. The presence of these states may greatly complicate the interpretation of ARPES experiments.

There is another feature of the ORTH structure that impacts the interpretation of ARPES data. Due to the cell doubling, the Cu-O barrel Fermi surface is centered at Γ. Of course it is centered as well at the Γ points of the neighboring Brillouin zones, including (in absolute reciprocal space) the locations where it is centered for the TET cell. On this basis it may be expected that ARPES experiments should see overlapping barrel Fermi surfaces. Away from the regions in the zone with Bi-O derived structure, these barrel Fermi surfaces are minimally perturbed, consistent with their observation by ARPES. However, there are matrix elements involved. One knows physically that as the ORTH displacements decrease in size towards the TET structure only one of the overlapping barrels will be seen. The point is that the "new" Γ centered barrels that arise in the ORTH structure will be

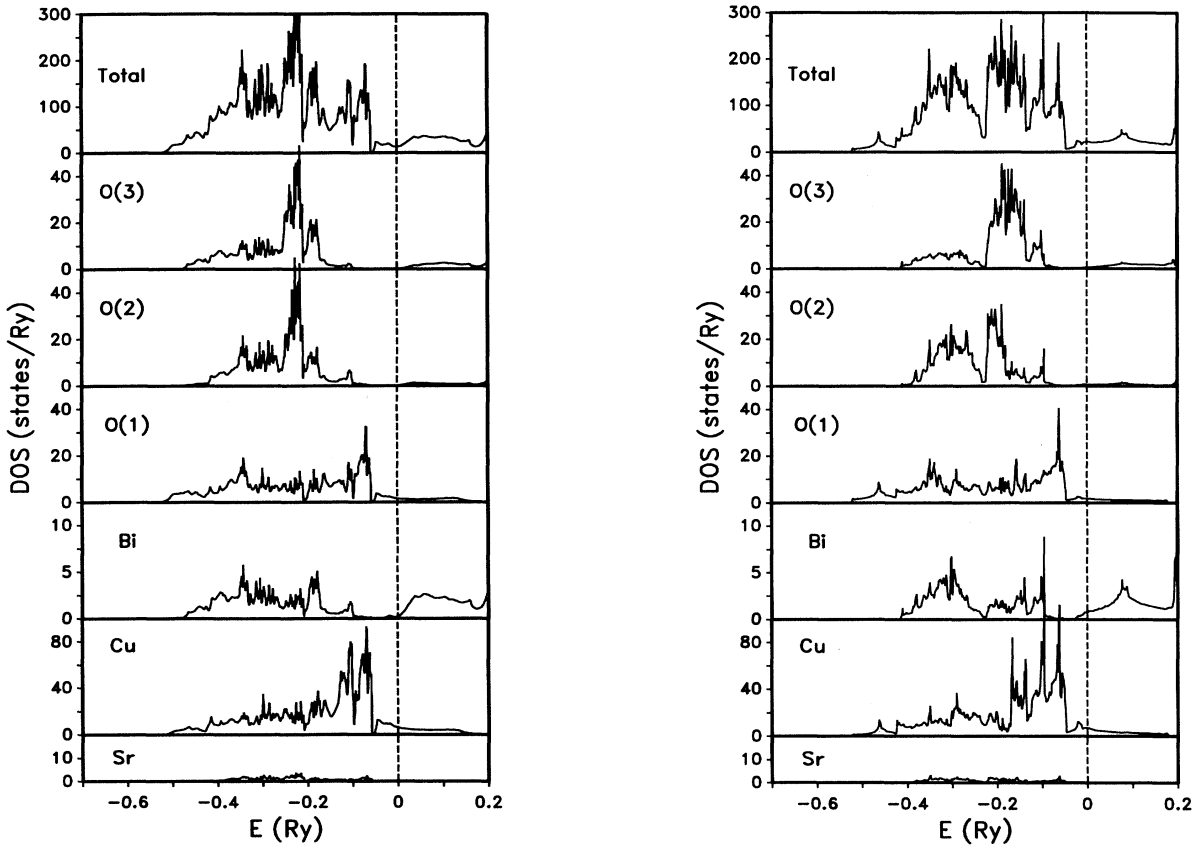

FIG. 5. Electronic DOS and projections for ORTH Bi2201 (left) and TET Bi2201 (right). The total DOS is per formula unit, while the projections are on a per atom basis and are the total DOS weighted by the contribution to the charge within the corresponding LAPW sphere.

evident in ARPES data to the extent that exiting photoelectrons are "umclapped" by the potential arising from the ORTH displacements. If the displacements could be decreased continuously, the intensity of the extra Γ centered barrels would vanish smoothly. However, in bismuth cuprates the ORTH modulation would seem strong enough that this folded barrel surface may contribute weak intensity and additional ambiguity to the interpretation of ARPES data. In this regard, Aebi *et al.*[7] report observing with ARPES a $c(2\times2)$ (i.e., $\sqrt{2}\times\sqrt{2}$) superstructure on the Fermi surface of Bi2212, which they ascribe to antiferromagnetic correlations. However, as in Bi2201, the structural distortions in Bi2212 consist of a $c(2\times2)$ ORTH-like displacement pattern and an additional incommensurate modulation. Accordingly, it seems that structural effects are a more probable cause of the observed weak $c(2\times2)$ Fermi-surface superstructure.

As mentioned Bi2212 has been the main focus of experimental investigations of the bismuth cuprate HTS. However, larger effects may be present in its electronic structure due to the stronger superstructure in that material. Detailed calculations of the effects of the incommensurate superstructure in Bi2212 will be extremely useful in sorting out its electronic structure, especially to distinguish fundamental aspects of the electronic characteristics of the superconducting cuprates from effects due simply to the modulation of the Bi-O layers in this particular compound.

ACKNOWLEDGMENTS

This work was supported in part by the Office of Naval Research. Computations were performed using the machines at the DoD high performance computing center at CEWES and the Arctic Region Supercomputer Center. We thank the authors of Ref. 34 for a copy of their work.

[1]W. E. Pickett, R. E. Cohen, H. Krakauer, and D. J. Singh, Science **255**, 46 (1992), and references therein.

[2]C. G. Olson, R. Liu, D. W. Lynch, R. S. List, A. J. Arko, B. W. Veal, Y. C. Chang, P. Z. Jiang, and A. P. Paulikas, Phys. Rev. B **42**, 381 (1990).

[3]T. Takahashi, H. Matsuyama, H. Katayama-Yoshida, Y. Okabe, S. Hosoya, K. Seki, H. Fujimoto, M. Sato, and H. Inokuchi, Phys. Rev. Lett. **39**, 6636 (1989).

[4]R. Manzke, T. Buslaps, R. Claessen, and J. Fink, Europhys. Lett. **9**, 477 (1989).

[5]Z.-X. Shen, D. S. Dessau, B. O. Wells, D. M. King, W. E. Spicer, A. J. Arko, D. Marshall, L. W. Lombardo, A. Kapitulnik, P. Dickinson, S. Doniach, J. DiCarlo, A. G. Loeser, and C. H. Park, Phys. Rev. Lett. **70**, 1553 (1993); D. S. Dessau, Z. X. Shen, D. M. King, D. S. Marshall, L. W. Lombardo, P. H. Dickinson, A. G. Loeser, J. DiCarlo, C. H. Park, A. Kapitulnik, and W. E. Spicer, Phys. Rev. Lett. **71**, 2781 (1993).

[6]R. J. Kelley, J. Ma, C. Quitmann, G. Margaritondo, and M. Onellion, Phys. Rev. B **50**, 590 (1994).

[7]P. Aebi, J. Osterwalder, P. Schwaller, L. Schlapbach, M. Shimoda, T. Mochiku, and K. Kadowaki, Phys. Rev. Lett. **72**, 2757 (1994).

[8]E. R. Ratner, Z. X. Shen, D. S. Dessau, B. O. Wells, D. S. Marshall, D. M. King, W. E. Spicer, J. L. Peng, Z. Y. Li, and R. L. Greene, Phys. Rev. B **48**, 10 482 (1993).

[9]Y. Gao, P. Lee, P. Coppens, M. A. Subramanian, and A. W. Sleight, Science **241**, 954 (1988); Y. Gao, P. Lee, J. Ye, P. Bush, V. Petricek, and P. Coppens, Physica C **160**, 431 (1989).

[10]C. H. Chen, D. J. Werder, S. H. Liou, H. S. Chen, and M. Hong, Phys. Rev. B **37**, 9834 (1988).

[11]V. Petricek, Y. Gao, P. Lee, and P. Coppens, Phys. Rev. B **42**, 387 (1990).

[12]A. Yamamoto, M. Onoda, E. Takyama-Muromachi, F. Izumi, T. Ishigaki, and H. Asano, Phys. Rev. B **42**, 4228 (1990).

[13]C. Patterson, P. D. Hatton, R. J. Nelmes, X. Chu, Y. F. Yan, and Z. X. Zhao, Supercond. Sci. Technol. **3**, 297 (1990).

[14]P. Bordet, J. J. Capponi, C. Chaillout, J. Chenavas, A. W. Hewat, E. A. Hewat, J. L. Hodeau, M. Marezio, J. L. Tholence, and D. Tranqui, Physica C **156**, 189 (1988).

[15]Y. LePage, W. R. McKinnon, J. M. Tarascon, and P. Barboux, Phys. Rev. B **40**, 6810 (1989).

[16]K. K. Fung, R. L. Withers, Y. F. Fan, and Z. X. Zhao, J. Phys.: Condens. Matter. **1**, L320 (1989).

[17]A. I. Beskrovnyi, M. Dlouha, Z. Jirak, and S. Vratislav, Physica C **171**, 19 (1990).

[18]H. Budin, O. Eibl, P. Pongratz, and P. Skalicky, Physica C **207**, 208 (1993).

[19]M. S. Hybertsen and L. F. Mattheiss, Phys. Rev. Lett. **60**, 1661 (1988).

[20]H. Krakauer and W. E. Pickett, Phys. Rev. Lett. **60**, 1665 (1988).

[21]P. A. Sterne and C. S. Wang, J. Phys. C **21**, L949 (1988).

[22]S. Massidda, J. Yu, and A. J. Freeman, Physica C **152**, 251 (1988); see also L. P. Chan, D. R. Harshman, K. G. Lynn, S. Massidda, and D. B. Mitzi, Phys. Rev. Lett. **67**, 1350 (1991).

[23]L. F. Mattheiss and D. R. Hamann, Phys. Rev. B **38**, 5012 (1988).

[24]F. Herman, R. V. Kasowski, and W. Y. Hsu, Phys. Rev. B **38**, 204 (1988).

[25]C. C. Torardi, M. A. Subramanian, J. C. Calabrese, J. Gopalakrishnan, E. M. McCarron, K. J. Morrissey, T. R. Askew, R. B. Flippen, U. Chowdhry, and A. W. Sleight, Phys. Rev. B **38**, 225 (1988).

[26]O. K. Andersen, Phys. Rev. B **12**, 3060 (1975); D. J. Singh, *Planewaves, Pseudopotentials and the LAPW Method* (Kluwer Academic, Boston, 1994), and references therein.

[27]S. H. Wei and H. Krakauer, Phys. Rev. Lett. **55**, 1200 (1985).

[28]D. Singh, Phys. Rev. B **43**, 6388 (1991).

[29]This corresponds to an interstitial wave-vector cutoff of 17.58 Ry. LAPW sphere radii of 2.10, 2.50, 1.90, and 1.55 a.u. were used for Bi, Sr, Cu, and O, respectively.

[30]The relation between the TET and ORTH cells is as follows: For the body-centered TET cell lattice vectors of $(a,0,0)$, $(0,a,0)$, and $(a/2,a/2,c/2)$ were used. In the same Cartesian coordinate system the ORTH lattice vectors were $(\sqrt{2}a_1,0,0)$, $(0,-a_2/\sqrt{2},c/2)$, and $(0,a_2/\sqrt{2},c/2)$, where a_1 and a_2 are very slightly different from a due to the orthorhombic distortion. The volume of the ORTH cell is double that of the TET cell. The corresponding reciprocal-lattice vectors for TET are $(2\pi/a,0,-2\pi/c)$, $(0,2\pi/a,-2\pi/c)$ and $(0,0,4\pi/c)$; for ORTH they are $(\sqrt{2}\pi/a_1,0,0)$, $(0,-\sqrt{2}\pi/a_2,2\pi/c)$, and $(0,\sqrt{2}\pi/a_2,2\pi/c)$.

[31]H. Heinrich, G. Kostorz, B. Heeb, and L. J. Gauckler, Physica C **224**, 133 (1994).

[32]J. Ren, D. Jung, M. H. Wangbo, J. M. Tarascon, Y. LePage, W. R. McKinnon, and C. C. Torardi, Physica C **159**, 151 (1989).

[33]E. R. Ratner, Z. X. Shen, D. S. Dessau, B. O. Wells, D. S. Marshall, D. M. King, W. E. Spicer, J. L. Peng, Z. Y. Li, and R. L. Greene, Phys. Rev. B **48**, 10 482 (1993).

[34]D. M. King, Z. X. Shen, D. S. Dessau, D. S. Marshall, C.H. Park, W. E. Spicer, J. L. Peng, Z. Y. Li, and R. L. Greene, Phys. Rev. Lett. **73**, 3298 (1994).